Inter-radar Interference Mitigation via Self-attention Augmented biGRU and Customized Loss Functions

Yudai SUZUKI
Graduate School of Science and Engineering
Ibaraki University
Hitachi, Japan
24nm630l@vc.ibaraki.ac.jp

Xiaoyan WANG
Graduate School of Science and Engineering
Ibaraki University
Hitachi, Japan
xiaoyan.wang.shawn@vc.ibaraki.ac.jp

Masahiro UMEHIRA
Department of Electronics and Communication Technology
Nanzan University
Nagoya, Japan
umehira@nanzan-u.ac.jp

Hao ZHOU
School of Computer Science
University of Science and Technology of China
Hefei, China
kitewind@ustc.edu.cn

***Abstract*—CS (Chirp Sequence) radars are one of the most essential sensors for perceiving the surrounding environment in automotive applications. However, as the number of radar sensors increases, inter-radar interference becomes more prevalent, leading to a severe degradation in target detection rates. To address this issue, we propose a self-attention augmented dual-channel biGRU model to mitigate wideband interference, and explore various customized loss functions to enhance its performance. Specifically, the dual-channel biGRU processes the real and imaginary components of the radar beat signal simultaneously, while multi-head self-attention enhances the model's focus on critical segments of the input signal. Additionally, the customized loss functions either incorporate both time and frequency domain information or utilize both interfered and interference-free samples to more effectively reconstruct the beat signal. The effectiveness of the proposed interference mitigation method is validated through extensive simulations, showing superior performance in terms of SNR (Signal-to-Noise Ratio), amplitude absolute error, phase absolute error, and F1 score compared to existing approaches.**

Keywords—CS radar, inter-radar interference, wideband interference, biGRU, self-attention, loss function

I. INTRODUCTION

Accurate sensing is crucial for ensuring the safety of autonomous driving. Compared with camera and LiDAR (Light Detection and Ranging), mmWave (millimeter wave) radar systems offer the benefits such as high resolution, cost-effectiveness, and resilience to diverse weather and lighting environments. Specifically, the CS (Chirp Sequence) radar [1] is a promising solution for automotive sensors, known for its ability to simultaneously measure the distances and velocities of multiple targets. However, with the widespread adoption of CS radars in mmWave frequency band, the probability of inter-radar interference [2] increases and is expected to become a significant concern in the near future.

The interference among CS radars can be divided into two categories depending on the victim and interference signals' chirp rates. When the chirp rate of interference radar differs from that of the victim radar, wideband interference (or known as non-coherent interference) occurs [3]. It will raise the noise floor in the frequency domain, resulting in lower target detection rates. In contrast, when the interference radar has the same chirp rate as the victim radar, narrowband interference (or known as coherent interference) occurs [4]. It will induce spurious peaks in the frequency domain, leading to false detection due to the ghost target. In this study, we focus on the wideband interference.

In recent years, various signal processing-based interference mitigation methods for automotive radar have been proposed. These approaches can be divided into two categories: 1) traditional signal processing algorithm and 2) deep-learning (DL) based signal reconstruction schemes. In category 1), the zero suppression method stands out as a simple approach that uses a time domain threshold to detect and zero-out interfered samples. Lee *et al.* proposed a wavelet denoising based approach [5] which estimates and extracts the interference component from corrupted signal by utilizing time-domain low-pass filter. In category 2), Ristea *et al.* proposed to use fully convolutional network (FCN) to transform interfered STFT (Short-Term Fourier-Transform) spectrum to interference-free frequency spectrum [6]. Mun *et al.* proposed an Attention-biGRU (bidirectional Gated Recurrent Units) based approach to mitigate interference and recover signal in time domain [7]. To consider phase information which is important for the post signal processing, Wang *et al.* proposed a complex-valued CNN (Convolutional Neural Network) method with prior feature as a regularization term [8].

In this paper, we propose a self-attention augmented dual-channel biGRU approach that simultaneously processes the real and imaginary parts of beat signals. Additionally, we explore customized loss functions to enhance the performance of the learning model. We conduct extensive simulations in multi-interference scenarios, and the results demonstrate the superiority of the proposed method in terms of SNR (Signal to Noise Ratio), amplitude AE (Absolute Error), phase AE, and F1 score compared with existing methods.

II. PRINCIPLES OF INTER-RADAR INTERFERENCE

A. Principle of Chirp Sequence Radar

Fig.1 shows the principle of the CS radar system. CS radar transmits sawtooth frequency-modulated signal continuously from the Tx antenna. The signal reflected from the target is received by the Rx antenna. The m -th transmitted and received chirp signals can be expressed by Eqns. (1) and (2), respectively.

$$s_{\mathrm{Tx}}(t,m) = A_{\mathrm{Tx}} \exp\left\{j2\pi\left(f_c(t-mT) + \frac{\Delta f}{\Delta T}(t-mT)^2\right)\right\} \quad (1)$$

$$s_{\mathrm{Rx}}(t,m) = A_{\mathrm{Rx}} s_{\mathrm{Tx}}(t-\tau,m) \quad (2)$$

$$\tau = \frac{2(R+Vt)}{c} \quad (3)$$

where $A_{\mathrm{Tx}}, A_{\mathrm{Rx}}$ are the transmitted and received signals' amplitude, f_c is start frequency, Δf is bandwidth, ΔT is

chirp duration, τ is time delay, R and V are relative distance and relative velocity of target, and c is light speed. The beat signal is obtained by dechirping and passing through a LPF (Low-Pass Filter). When ΔT is extremely short, the beat frequency f_b and the Doppler frequency f_d are represented by Eqns. (4) and (5), respectively.

$$f_b = \frac{\Delta f}{\Delta T}\cdot\frac{2R}{c} + \frac{2V}{c}f_c \cong \frac{\Delta f}{\Delta T}\cdot\frac{2R}{c}, \quad \left(if\ \frac{\Delta f}{\Delta T}\cdot\frac{2R}{c} \gg \frac{2V}{c}f_c\right) \tag{4}$$

$$f_d = \frac{2V}{c}f_c \tag{5}$$

Subsequently, range-Doppler processing is applied to the beat signal, generating the range-Doppler (RD) map. The peak in the RD map reveals the beat frequency, enabling the computation of the target's range and velocity using Eqns. (6) and (7).

$$R = \frac{c\Delta T}{2\Delta f}f_b \tag{6}$$

$$V = \frac{c}{2f_c}f_d \tag{7}$$

B. Principle of Wideband Interference

As illustrated in Fig. 2, when a radar receives an aggressor signal with a different chirp rate, wideband inter-radar interference occurs. The interfered beat signal could be expressed in Eqn. (8).

$$y(t) = s_b(t) + n(t) + s_{int}(t) \tag{8}$$

where $s_b(t)$ is the desired beat signal, $n(t)$ is the noise, and $s_{int}(t)$ is the interference signal. Fig. 3 illustrates the wideband interference in both the time and frequency domains. The power of the signal received from the aggressor radar typically exceeds that of the desired signal. Therefore, a pulsed interference pattern emerges when analyzed in the time domain and the spectral noise floor is elevated due to the presence of interference. As a result, the raised noise floor may lead to missed detection of the targets.

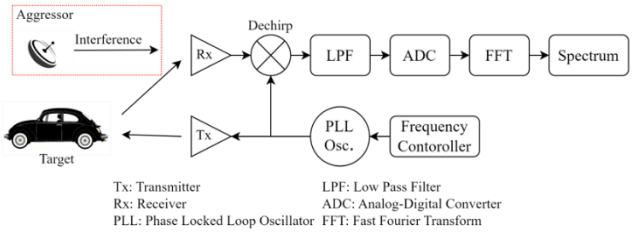

Fig. 1 Block diagram of CS radar system

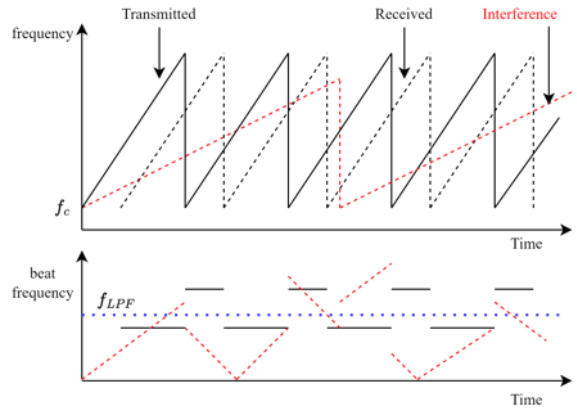

Fig. 2 Wideband interference of CS radar system

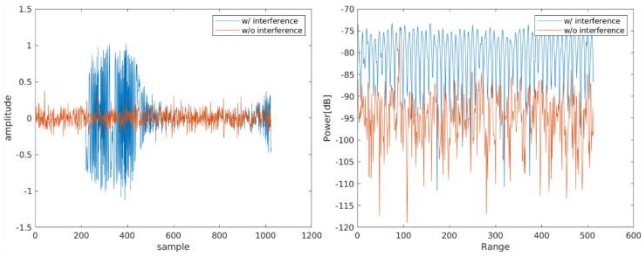

Fig. 3 Time waveform and range profile of the beat signal with and without interference

III. Proposed Interference Mitigation Method

A. Self-Attention Augmented Dual-channel biGRU

Our goal is to design and develop a neural network that can effectively mitigate wideband interference by transforming an interfered beat signal input into a clean, interference-free beat signal output. This network is designed to handle complex interference patterns across a broad frequency range, making it robust in challenging and complex environments. To achieve this, we propose a self-attention augmented dual-channel biGRU architecture as illustrated in Fig. 4. The network's input consists of the real and imaginary parts of the interfered beat signals in the time domain, while the output is the beat signals after interference suppression.

It comprises three dual-channel biGRU layers, which are responsible for capturing both forward and backward dependencies of the signal. These layers process the real and imaginary parts of the input beat signal separately, ensuring that each component is handled independently to preserve the integrity of the original signal. Noted that the models based on Vanilla RNN (Recurrent Neural Network) and LSTM (Long Short-Term Memory) are evaluated on our previous work [9], and the results showed that GRU cell is the most cost-efficient one. Additionally, the network features multi-head self-attention mechanisms [10], which is widely used in deep learning models especially in natural language processing and computer vision. Two self-attention layers, each with 4 heads, are designed to capture intricate relationships and dependencies between different signal components. By combining the outputs of the preceding biGRU layers, the self-attention mechanism enhances the model's ability to focus on critical features across the entire signal, ensuring that both local and global patterns are effectively learned. This layered approach allows the network to achieve superior interference mitigation compared to traditional methods.

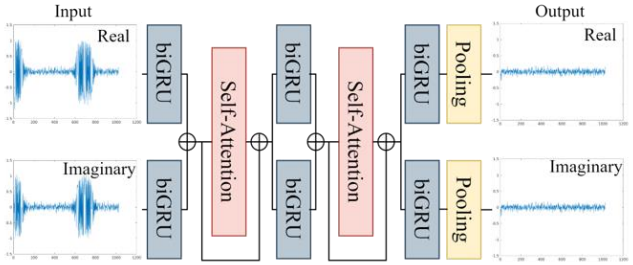

Fig. 4 Architecture of the proposed self-attention augmented dual-channel biGRU model

B. Loss Functions

The optimization of the neural network relies heavily on the choice of loss functions. To improve the performance on interference mitigation, we explore four different types of loss functions: time domain mean squared error (MSE) loss, frequency domain phase MSE loss, frequency domain amplitude MSE loss, and a contrastive learning-driven loss function.

1) Time domain MSE

The time domain MSE loss function includes both real and imaginary parts of the signals, which is calculated by Eqn. (9):

$$l_{time} = \frac{1}{N}\left\{\begin{array}{l}\sum_{t=1}^{N}\left(\mathcal{R}\left(\hat{y}(t)\right)-\mathcal{R}\left(y(t)\right)\right)^2 \\ +\sum_{t=1}^{N}\left(\mathcal{I}\left(\hat{y}(t)\right)-\mathcal{I}\left(y(t)\right)\right)^2\end{array}\right\} \quad (9)$$

where N is the total number of time samples, $\mathcal{R}(\cdot)$ and $\mathcal{I}(\cdot)$ are real and imaginary parts, $\hat{y}(t)$ is the label, i.e. interference-free signal in the time domain, and $y(t)$ is the predicted signal in the time domain. This loss function focuses on the features in the time domain and aims to produce a beat signal waveform as close as possible to the interference-free one.

2) Frequency domain phase MSE

To account for frequency domain phase information during training, we introduce the phase MSE loss function, as given by Eqn. (10):

$$l_{phase} = \frac{1}{N}\sum_{f=1}^{N}\left\{\text{atan}\left(\frac{\mathcal{I}\left(\hat{Y}(f)\right)}{\mathcal{R}\left(\hat{Y}(f)\right)}\right)-\text{atan}\left(\frac{\mathcal{I}\left(Y(f)\right)}{\mathcal{R}\left(Y(f)\right)}\right)\right\}^2 \quad (10)$$

where $\hat{Y}(f)$ and $Y(f)$ denote the Fourier transforms of $\hat{y}(t)$ and $y(t)$, respectively. This loss function measures the MSE of phase information in the frequency domain, it helps in optimizing the model to accurately reconstruct the phase information which is crucial for the upcoming signal processing.

3) Frequency domain amplitude MSE

The frequency domain amplitude MSE loss function, computed by Eqn. (11), provides MSE between the frequency spectrum amplitude of the label and that of prediction.

$$l_{amplitude} = \frac{1}{N}\sum_{f=1}^{N}\left\{abs\left(\hat{Y}(f)\right)-abs\left(Y(f)\right)\right\}^2 \quad (11)$$

This loss function focuses on preserving the peak and noise levels in the frequency domain.

4) Time domain contrastive loss

The contrastive strategy enables the model to learn by moving the predictions closer to the positive samples and further away from the negative samples. In this work, the time domain interference-free beat signals are treated as the positive samples, while the time domain interfered beat signals serve as the negative samples. The model is trained to minimize the distance between the predicted signal and the interference-free signal, while simultaneously maximizing the distance from the corrupted signals. This feature is captured by the contrastive loss, which is defined in Eqn. (12).

$$l_{contrastive} = \frac{MSE\left(\mathcal{R}\left(\hat{y}(t)\right),\mathcal{R}\left(y(t)\right)\right)}{MSE\left(\mathcal{R}\left(x(t)\right),\mathcal{R}\left(y(t)\right)\right)} + \frac{MSE\left(\mathcal{I}\left(\hat{y}(t)\right),\mathcal{I}\left(y(t)\right)\right)}{MSE\left(\mathcal{I}\left(x(t)\right),\mathcal{I}\left(y(t)\right)\right)} \quad (12)$$

where $x(t)$ is the interfered beat signal, i.e. the input data. This loss function utilizes both interfered and interference-free samples, aiming to ensure that interference-free and interference-suppressed signals are close together, and interfered and interference-suppressed signals are far apart.

C. Learning model generation

In this work, we explore the proposed model with 4 different loss functions, i.e., a straightforward time MSE loss function given in Eqn. (9), as well as 3 customized loss functions as follows.

- Time + phase (Eqn. (9) + Eqn. (10))
- Time + phase + amplitude (Eqn. (9) + Eqn. (10) + Eqn. (11))
- Contrastive (Eqn. (12))

The ADAM optimizer is employed with a learning rate of 0.001 and a batch size of 128. The training procedure is run for 100 epochs using an Nvidia RTX A6000 GPU. We randomly generate 50 pairs of interfered and interference-free scenarios, each consisting of 75 chirps. Therefore, the total data size for training is 3750 samples. The random ranges of the radar parameters are shown in Table 1.

Table. 1 Radar Parameters

Parameters	min	max
Center frequency	76	78
Distance	1m	130m
Velocity	1km/h	50km/h
Chirp duration	25	50
Bandwidth	100MHz	200MHz
Number of targets	1	1
Number of interferences	1	4

IV. Performance Evaluation

In this section, we present the performance evaluation of the proposed self-attention augmented dual-channel biGRU model with customized loss functions, and compare it against the existing wavelet denoising method (WD) [5] and attention-biGRU approach [7].

To showcase the interference suppression capabilities of the proposed method, the examples of waveforms and RD maps, both with and without interference, as well as after interference mitigation by each approach, are shown in Figs. 5 and 6. From Fig. 5, it is evident that the waveform with interference exhibits clear pulsed-like interference signals. The WD method can eliminate interference samples, however, it also damages the target's signal samples. In contrast, both the attention-biGRU model and the proposed methods effectively reconstruct the corrupted samples, with the signal reconstructed by the proposed methods being much closer to the interference-free signal. From Fig. 6, we observe that the target peak completely disappears due to

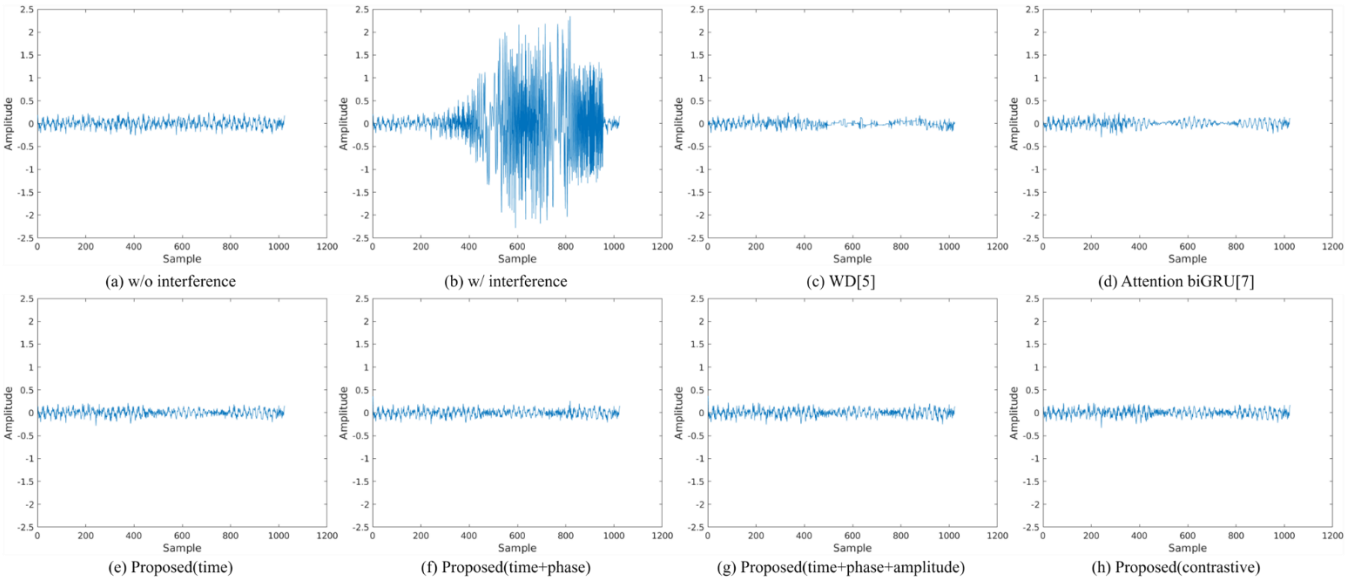

Fig. 5 Time waveform

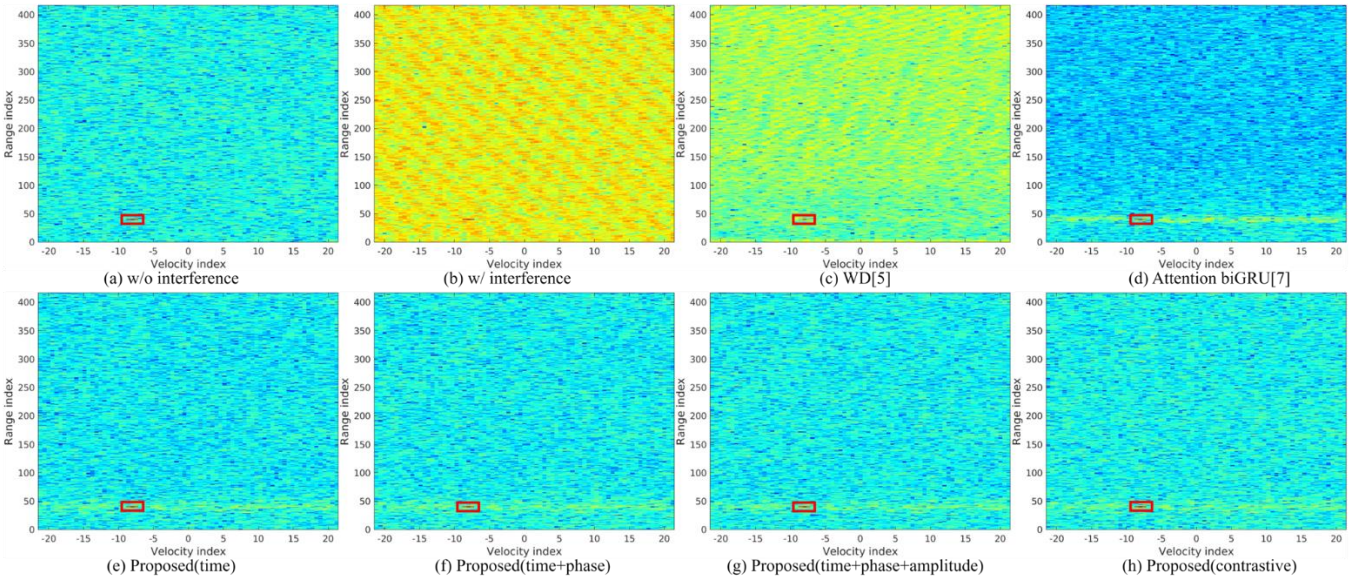

Fig. 6 Range-Doppler map

the elevated noise floor when the interference occurs. The WD method performs poorly, especially in the high-frequency region. In contrast, both the attention-biGRU model and the proposed methods effectively suppress the interference. The proposed methods with customized loss functions (shown in Figs. 6(f)~(h)), demonstrate superior performance.

To quantitatively evaluate the interference mitigation performance, we measured the signal-to-noise ratio (SNR) as well as the amplitude absolute error (AE), phase AE for the targets, and F1 score, using 25 randomly generated test scenarios. Fig. 7 depicts the cumulative distribution function (CDF) of the SNR across different interference mitigation methods. The proposed methods with customized loss functions consistently outperform the WD and attention-biGRU methods and keep a relatively small gap from the result without interference.

Figs. 8 and 9 depict the amplitude and phase AE of the targets, indicating the signal recovery capabilities of different methods. Both the WD and attention-biGRU methods exhibit relatively high amplitude AE, but the attention-biGRU method is more effective at handling phase AE compared to WD. The proposed methods with customized loss functions demonstrate superior performance in both amplitude and phase AE. Specifically, compared with existing methods, the amplitude AE below 5dB and phase AE below 10 degrees increases by at least 20% and 10%, respectively.

Finally, Table 2 summarizes the F1 score and processing time across different methods. The cell-average continuous false detection rate algorithm (CA-CFAR) was employed for target detection. It was set with 14 guard cells and 237 training cells and the probability of false alarm of 1×10^{-4}. It is shown that the proposed method with time + phase + amplitude loss function outperforms the WD [5] and attention-biGRU [7] in terms of F1 score by approximately 38%. However, as expected, this performance improvement comes with a longer processing time.

V. Conclusions

In this work, we propose a self-attention augmented dual-channel biGRU model to mitigate the inter-radar wideband interference, and explore various customized loss functions to enhance its performance. The effectiveness of the proposed method is validated through extensive simulations with synthetic radar signals. Our future work will involve assessing the performance of the proposed method with real-world experimental radar signals.

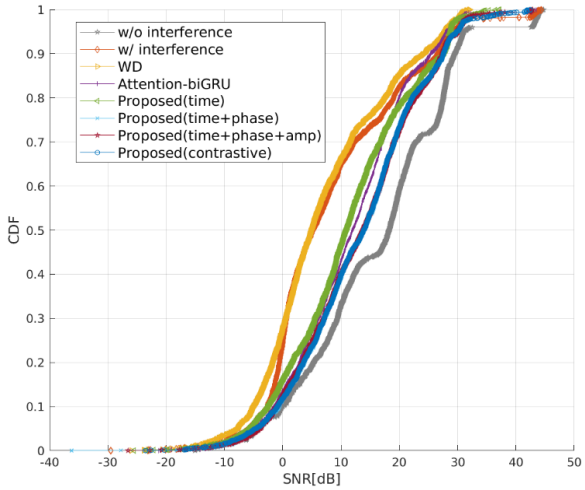

Fig. 7 CDF of SNR

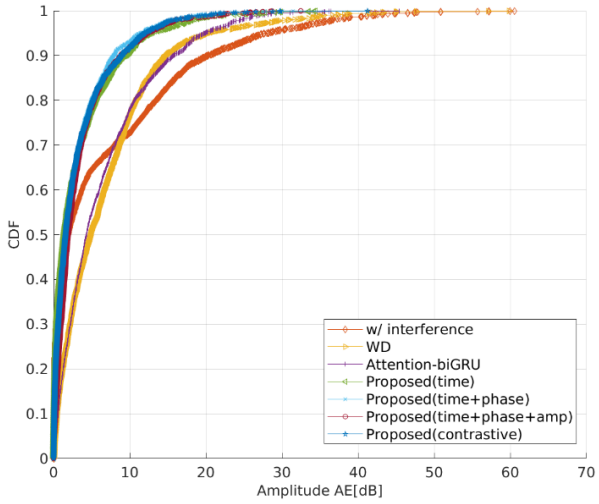

Fig. 8 CDF of amplitude AE

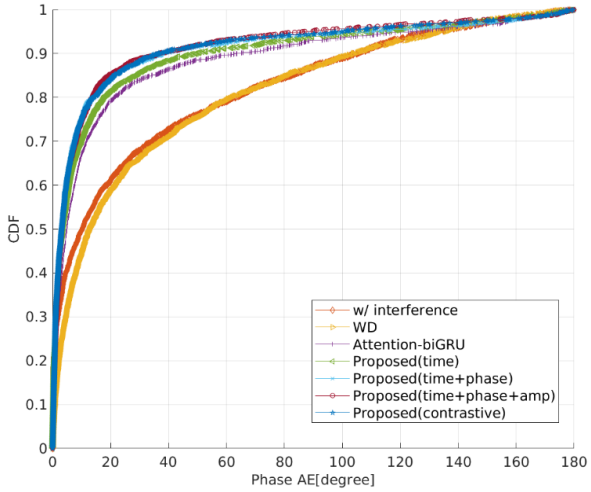

Fig. 9 CDF of phase AE

Table. 2 F1 score and processing time

	F1 score	Processing time [msec]
w/ interference	0.485	-
WD [5]	0.611	5.20
Attention-biGRU [7]	0.615	30.2
Proposed (time)	0.677	42.8
Proposed (time+phase)	0.710	43.0
Proposed (time+phase+amplitude)	**0.846**	**45.0**
Proposed (contrastive)	0.647	45.6

Acknowledgment

This research and development work was supported by the MIC/SCOPE ## JP225003006.

References

[1] C. Waldschmidt, J. Hasch and W. Menzel, "Automotive Radar — From First Efforts to Future Systems," in IEEE Journal of Microwaves, vol. 1, no. 1, pp. 135-148, Jan. 2021.J. Clerk Maxwell, A Treatise on Electricity and Magnetism, 3rd ed., vol. 2. Oxford: Clarendon, 1892, pp.68–73.

[2] M. Umehira, Y. Watanabe, X. Wang, S. Takeda and H. Kuroda, "Inter radar interference in automotive FMCW radars and its mitigation challenges," 2020 IEEE International Symposium on Radio-Frequency Integration Technology (RFIT), 2020, pp. 220-222.

[3] X. Wang, R. Koizumi, M. Umehira, R. Sun, and S. Takeda, "Wideband Interference Suppression for Automotive mmWave CS Radar: From Algorithm-based to Learning-based Approaches", IEICE Transactions on Communications, Vol.E107-B,No.12,pp.-,Dec. 2024.

[4] M. Umehira, Y. Takeuchi, X. Wang, "Adaptive Interference Mitigation for Time-varing Narrowband Interference in Automotive CS Radars", Proc. of the International Radar Conference (RADAR 2024), 21-25 October 2024.

[5] Lee S, Lee J Y, Kim S C., ”Mutual interference suppression using wavelet denoising in automotive FMCW radar systems,” IEEE Trans. Intell. Transp. Syst., vol. 22, no. 2, pp. 887-897, Feb. 2021.

[6] N.-C. Ristea, A. Anghel, and R. T. Ionescu, ‘‘Fully convolutional neural networks for automotive radar interference mitigation,’’ in Proc. IEEE 92nd Veh. Technol. Conf. (VTC-Fall), Nov. 2020, pp. 1–5.

[7] J. Mun, S. Ha, and J. Lee, “Automotive radar signal interference mitigation using RNN with self attention,” in Proc. IEEE Int. Conf. Acoust., Speech Signal Process. (ICASSP), May 2020, pp. 3802–3806.

[8] J. Wang, R. Li, Y. He and Y. Yang, ”Prior-Guided Deep Interference Mitigation for FMCW Radars,” IEEE Trans. Geosci. Remote Sens., vol. 60, pp. 1-16, 2022.

[9] Y. Suzuki, X. Wang, M. Umehira, R. Sun and S. Takeda, "Performance and Inference Time Tradeoff for RNN Model Based Wideband Inter-Radar Interference Mitigation", Proc. of International Conference on Ubiquitous and Future Networks (ICUFN 2024), 2-5 July 2024.

[10] A. Vaswani, N. Shazeer, N. Parmar, J. Uszkoreit, L. Jones, A. N. Gomez, Ł. Kaiser, and I. Polosukhin. 2017. “Attention is all you need” In Proceedings of the 31st International Conference on Neural Information Processing Systems (NIPS'17). Curran Associates Inc., Red Hook, NY, USA, 6000–6010